Universal mechanism for breaking amide bonds by ionizing radiation

Phillip S. Johnson,[1] Peter L. Cook,[1] Xiaosong Liu,[2] Wanli Yang,[2] Yiqun Bai,[3] Nicholas L. Abbott,[3] and F. J. Himpsel[1,a)]
[1]*Department of Physics, University of Wisconsin-Madison 1150 University Ave., Madison, Wisconsin 53706, USA*
[2]*Advanced Light Source, Lawrence Berkeley National Laboratory Berkeley, California 94720, USA*
[3]*Department of Chemical and Biological Engineering, University of Wisconsin-Madison, 1415 Engineering Drive, Madison, Wisconsin 53706, USA*

(Received 12 April 2011; accepted 28 June 2011; published online 25 July 2011)

The photodissociation of the amide bond by UV light and soft x-rays is investigated by x-ray absorption spectroscopy at the C, N, and O 1s edges. Irradiation leaves a clear and universal signature for a wide variety of amides, ranging from oligopeptides to large proteins and synthetic polyamides, such as nylon. As the π^* peak of the amide bond shrinks, two new π^* peaks appear at the N 1s edge with a characteristic splitting of 1.1 eV. An additional characteristic is the overall intensity reduction of both the π^* and σ^* features at the O 1s edge, which indicates loss of oxygen. The spectroscopic results are consistent with the release of the O atom from the amide bond, followed by the migration of the H atom from the N to one of its two C neighbors. Migration to the carbonyl C leads to an imine, and migration to the C_α of the amino acid residue leads to a nitrile. Imine and nitrile produce the two characteristic π^* transitions at the N 1s edge. A variety of other models is considered and tested against the N 1s spectra of reference compounds. © *2011 American Institute of Physics*. [doi:10.1063/1.3613638]

I. INTRODUCTION

The amide bond plays a central role in protein chemistry. It forms the backbone of proteins by linking amino acids and thus determines the chemical stability of all forms of life.[1] In this context it is referred to as the peptide bond. Beyond protein chemistry one finds the amide bond in many other areas of organic chemistry. For example, it forms polyamides, a widely used class of polymers containing nylons and Kevlar.

The effect of ionizing radiation (UV, x-rays, gamma rays, cosmic rays, electrons) on biomolecules and polymers[2] has been of great interest for many reasons. Examples are radiation-induced mutations, UV-induced skin cancer, radiation therapy, irradiation of food for sterilization, photoresists in UV and EUV lithography,[3] radiation damage by x-rays in protein crystallography,[4–6] proteomics via electrospray ionization,[7] radiation damage of biological samples in microscopy,[8–11] photo-degradation of polymers by sunlight or x-rays,[12–14] degradable polymers to reduce plastic waste, and the role of radiation in forming the chemical building blocks of life.[15,16]

More specifically, radiation damage of proteins in aqueous environments is frequently explained as a two-step process. The primary photochemical process splits water, and the resulting fragments attack the peptide bond in a secondary reaction. Direct processes come into play only at low temperatures.[5] Non-biological polyamides, such as nylons and Kevlar, are susceptible to photo-degradation by the UV component of sunlight[13] (Kevlar more so than nylon because its aromatic components absorb near-UV light). A variety of models for specific photodissociation processes has been developed.[4,17–22]

Radiation damage studies of DNA (Refs. 23 and 24) have identified dehydrogenation of the monomers (i.e., the nucleotide bases) as a common reaction, leading to the formation of thymine dimers, which can cause skin cancer. This process can be induced by low energy electrons (~2 eV), which are a byproduct of the cascade of secondary electrons that accompanies ionizing radiation in tissue.

In studies of photochemistry at surfaces there have been efforts to find a generic mechanism for photon-stimulated desorption that is applicable to a broad class of materials. Among the proposed mechanisms are optical transitions to repulsive potential curves[25,26] and Coulomb repulsion in ionic crystals after the conversion of a negative ion into a positive ion by an Auger process.[27] Indirect dissociation by secondary electrons has been considered as well.[28]

Here we report a universal photochemical bond breaking pattern of amides, which leaves a characteristic fingerprint at the N 1s x-ray absorption edge in the form of two low-lying π^* transitions. This occurs for all amides that we have studied, ranging from amino acid dimers all the way to large proteins and polyamides. It also occurs over a wide photon energy range of at least 11–600 eV. Such a widespread phenomenon suggests a universal mechanism for the attack of the amide bond by ionizing radiation which may be explained by the involvement of secondary electrons created by the primary photoexcitation.

Previously proposed models for radiation damage of amides by soft x-rays[9,11,29] together with many other conceivable models are tested systematically using reference

a)Author to whom correspondence should be addressed. Electronic mail: fhimpsel@facstaff.wisc.edu.

compounds. Only one of many models is consistent with all the x-ray absorption data at the C, N, and O 1s edges. First, the oxygen atom is removed from the amide bond, then a H atom moves from the N to one of the two neighboring C atoms (either C or C_α), forming either an imine or a nitrile. These results illustrate the ability of soft x-ray spectroscopy to identify biochemical reactions involving proteins, including the effect of radiation damage.

II. SAMPLE PREPARATION

All chemicals were obtained from Sigma-Aldrich in anhydrous powder form and used as received. Two general methods were used to prepare the samples. One consisted of rubbing the powder into conductive carbon tape, the other of drop casting a dilute solution on a Si wafer covered either with native oxide or Au. The latter has the advantage of obtaining meaningful C 1s spectra but the possible drawback of incorporating reaction products with the solvent into the sample. Since many of the samples are insulating, a fine distribution of the powder in the tape or a sufficiently thin film is important to prevent instabilities in the absorption spectra when measured in the total electron yield mode.

Specifically, the samples whose spectra are shown in the figures were prepared as follows: Cytochrome c, cytosine, melamine, polyacrylonitrile, dimethyl cyclohexadiene diylidene biscyanamide, 4,6-dihydroxypyrimidine, and dimethyl adipimidate·2 HCl (DMA) were pressed into carbon tape; alanine anhydride, hexaglycine, polyglycine, bovine serum albumin (BSA), and tris-pyridyl triazine were dissolved in deionized water and dried onto a silicon wafer; nylon 6 was dissolved in trifluoro ethanol and dried onto a silicon wafer; ethyl violet was dissolved in ethanol and dried onto a silicon wafer; and 8CB was dissolved in toluene and deposited onto a gold-coated silicon wafer. Because of its volatility, 6-nitroso-1,2-benzopyrone was evaporated onto a liquid nitrogen cooled copper rod.

In order to minimize secondary photochemical reactions involving waters of hydration and solvents, the samples were dried by pumping down to ultrahigh vacuum (10^{-10} Torr range) for several hours. Nevertheless, it is quite possible that the biological samples still contained a residual amount of waters of hydration which were bound too strongly to be pumped away. For example, cytochrome c contained about 5%–10% water as shipped. The O 1s absorption spectra of BSA in Fig. 2(b) show a small feature at ≈535 eV that coincides with the hydroxyl σ^* peak near 535 eV.[30] Nylon 6 does not have any feature at this energy in Fig. 2(c) because it contains very little water. In all cases the π^* peak of the amide bond completely dominates possible water-related features. Water does not have any absorption peaks in the O 1s π^* region.[30]

III. X-RAY ABSORPTION MEASUREMENTS

The x-ray absorption experiments were performed at the Synchrotron Radiation Center (SRC) in Madison and at the Advanced Light Source (ALS) in Berkeley. Details have been described previously.[31,32] Radiation damage was minimized by working with the narrowest possible monochromator slits, using filters (at the SRC), or spreading the light out over an area of 3×5 mm^2 (at the ALS). All absorption spectra were measured by collecting the total electron yield.

The photon energy was calibrated at the N 1s and O 1s edges by using the sharp 2p-to-3d transition in TiO_2 (rutile) at 458.0 eV as secondary standard. This value was established by measuring TiO_2 powder side-by-side with gas phase N_2 trapped inside an irradiated imide.[33] The first vibrational line of N_2 at 400.9 eV (Ref. 34) served as primary standard. The C 1s edge was calibrated to the 1s-to-π^* transition in graphite at 285.35 eV. The absolute accuracy is about ±0.2 eV, the relative accuracy between different compounds about ±0.1 eV, and the relative accuracy between different π^* peaks at the same absorption edge about ±0.05 eV. The energy resolution was significantly better than the width of the observed features, with the vibrational splitting of N_2 at the N 1s edge clearly resolved.

All spectra are normalized to the incident photon flux. In order to remove the effects of beam fluctuations and decay, the sample current is divided by the current from a mesh coated in situ with Au. After this division a linear background is subtracted using an extrapolation of the pre-edge signal. This background reflects absorption from valence states and lower-lying core levels. This normalization produces a signal proportional to the density of C, N, or O atoms which can be used to investigate photon-induced desorption.

The radiation dose (in Gy = J/kg) is determined by the following formula:

$$Dose = \left(\frac{I \cdot t}{Y_{Au}}\right)\left(\frac{1-F}{F}\right)\left(\frac{E}{V \cdot \rho}\right),$$

where I is the photocurrent from the Au mesh, t is the exposure time, Y_{Au} is the photoelectric yield of Au (which we assume to be 10% at ∼400 eV (Ref. 32)), F is the fraction of photons intercepted by the mesh (∼10%), E is the energy per photon, V is the irradiated volume of the sample, and ρ is the density of the sample. The volume is 1 mm^2 × 0.5 μm (spot size times absorption length) and the density is 1.35 g/cm^3 for BSA.[35] We find substantial variations in the sensitivity to irradiation between the different amides in Fig. 1 but did not explore them systematically, hence only dosage information for BSA is presented. The dosages for the two irradiated BSA spectra in Fig. 1 are 12 and 47 MGy, respectively. Comparable spectra were obtained in Ref. 9 (Fig. 8) for a bacterial surface protein at exposures of ∼13 MGy and ∼52 MGy.

IV. UNIVERSAL PATTERN OF BOND BREAKING

In order to characterize the photochemical reactions during irradiation of the amide bond, we use x-ray absorption spectroscopy as element- and orbital-selective technique. Since the amide bond orbital extends over the three atoms C, N, and O, one can use the corresponding 1s absorption edges for testing potential bond-breaking models in great detail. In these measurements, electrons are promoted from the 1s core levels into the lowest unoccupied valence orbitals, which typically have π^* character. The π^* orbital of the amide bond produces the most pronounced peak in the x-ray absorption spectra of amides[9,31,32,36–43] at all three absorption edges.

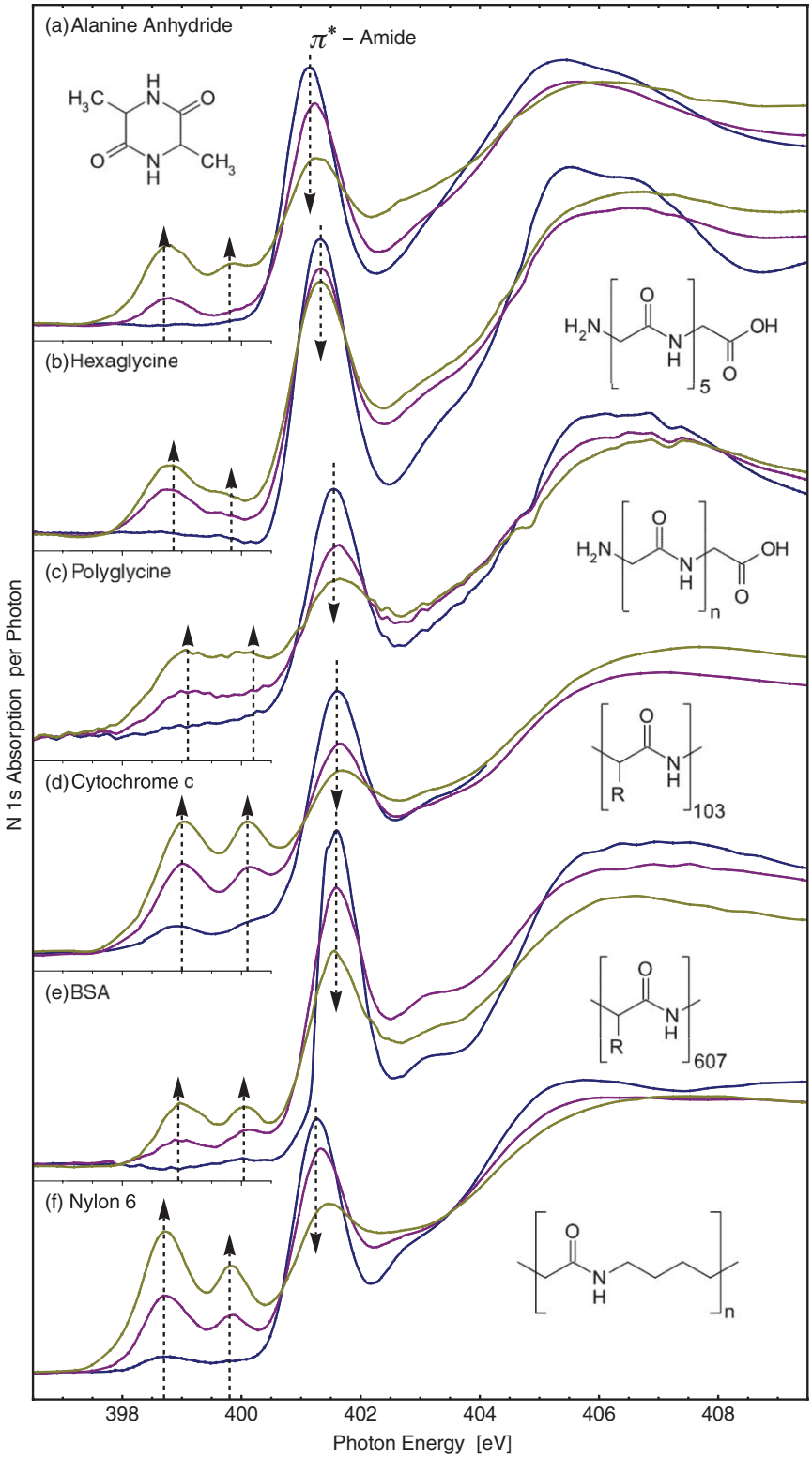

FIG. 1. N 1s absorption spectra versus irradiation for a variety of amides. Arrows indicate increasing radiation exposure. (a) Alanine anhydride, (b) hexaglycine, (c) polyglycine, (d) cytochrome c, (e) bovine serum albumine (BSA), and (f) nylon 6. In all cases, the characteristic π^* orbital of the amide bond at about 401.4 eV is quenched, and two new π^* orbitals appear at about 398.9 eV and 400.0 eV. That suggests a universal bond breaking mechanism.

The N 1s absorption edge is particularly selective of the amide bond. The optical matrix element between the N 1s core level and the π^* orbital selects the N atom at the center of the amide bond and eliminates any other C-, O-, or H-based bonds. Furthermore, this π^* orbital is not present in individual amino acids. It appears only after the formation of the peptide bond between amino acids.[37,38,42]

Figure 1 shows N 1s absorption spectra from a variety of amides, ranging from small molecules to polymers and encompassing both biological and non-biological compounds.

The pristine spectra all exhibit a major peak at about 401.4 eV that is due to the transition from the N 1s core level into the antibonding π^* orbital of the amide bond. The energy position of this π^* peak varies slightly between the different compounds in Fig. 1 (from 401.2 eV for the smallest molecules to 401.6 for BSA and cytochrome c). This can be attributed to different amino acid residues or to variations in the hydrogen bonding.

Upon irradiation with soft x-rays the π^* peak of the amide bond decreases and is gradually replaced by a pair of lower energy π^* peaks at about 398.9 eV and 400.0 eV. A small variation of the peak positions is observed among different compounds, similar to that for the pristine amide π^* peak. The splitting of the radiation-induced π^* doublet does not vary within the experimental accuracy of ± 0.05 eV and thus provides a rather stringent criterion for identifying the end product of the photochemical reaction. Another criterion is the intensity ratio of about 1.1 ± 0.1, with the more intense peak at 398.9 eV.

Similar observations have been made for bacterial surface proteins,[9] fibrinogen,[11] cytochrome c,[32] and various polypeptides.[40] A surprisingly similar doublet of low-lying π^* peaks has also been observed for amino acids after irradiation,[29,44] even though pristine amino acids do not exhibit the π^* peak of the peptide bond.[37,38] This has been explained by a polymerization of amino acids into peptides under irradiation.[29]

This characteristic radiation damage occurs over a wide photon energy range. We observe the effect from below 11 eV (the LiF window cutoff[45]) to at least 600 eV. The quantum efficiency is roughly proportional to the photon energy, which in turn is roughly proportional to the number of secondary electrons produced by a photon. This observation provides another argument for the involvement of secondary electrons in the radiation damage, rather than the primary photoabsorption event. This is reasonable, since the decay of a core hole produces only a single Auger electron but many secondary electrons. The end product must be rather stable, since the characteristic π^* doublet remains unchanged for at least 3 days in vacuum.

This photochemical bond breaking pattern happens consistently in a broad class of materials that have the amide bond as common feature. It is independent of whether the molecules are large or small, or whether or not they are biological. For example, the size range of the molecules covered in Fig. 1 starts with the shortest possible amides which are formed by a closed loop of two amino acids containing 2 amide bonds in alanine anhydride (Fig. 1(a)). Similar spectra are obtained from glycine anhydride (not shown). Next comes a short peptide (hexaglycine) containing 5 peptide bonds (Fig. 1(b)), a long peptide (polyglycine) containing several tens of peptide bonds (Fig. 1(c)), then the small protein cytochrome c with 103 peptide bonds (Fig. 1(d)), and eventually the large protein bovine serum albumin (BSA) containing 607 peptide bonds (Fig. 1(e)). Non-biological polyamides such as nylon 6 (Fig. 1(f)) exhibit the same spectroscopic pattern.

In order to provide additional information about the bond-breaking pattern, we use the O 1s edge in Fig. 2 and

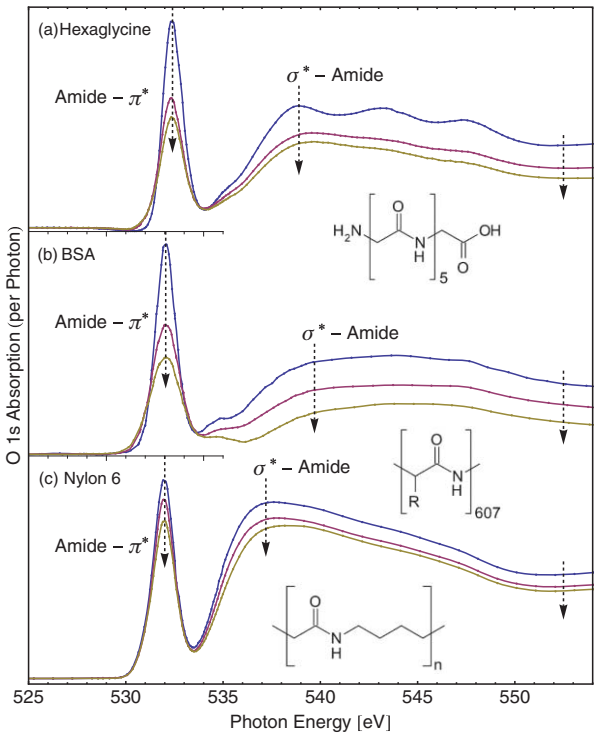

FIG. 2. O 1s absorption spectra versus irradiation for hexaglycine, BSA, and nylon 6. The π^* and σ^* peaks both decay with irradiation. This indicates removal of oxygen from the amide bond. The amide π^* orbital at ≈532.2 eV includes the C=O double bond.

the C 1s edge in Fig. 3. Like at the N 1s edge, the prominent peak in the pristine spectra corresponds to a transition into the π^* orbital of the amide bond (≈532.2 eV for O 1s, ≈401.4 eV for N 1s, ≈288.1 eV for C 1s). This reflects the fact that the amide bond extends over all three atoms.

A closer look at the character of the amide bond and its implications on the x-ray absorption spectra is given in Figs. 4(a1) and 4(a2). The amide bond is a conjugated π system which can be viewed as a superposition of a

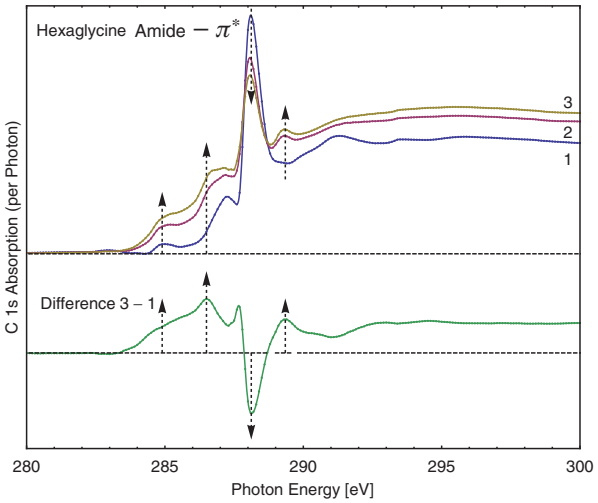

FIG. 3. C 1s absorption spectrum of hexaglycine versus irradiation. The π^* peak of the amide bond at 288.1 eV decays with irradiation. Since this π^* orbital includes the C=O bond, its decay confirms the removal of oxygen. The difference spectrum reveals the appearance of extra features below the amide π^*. Two arrows at 284.9 eV and 286.5 eV indicate typical positions of imine and nitrile π^* transitions.

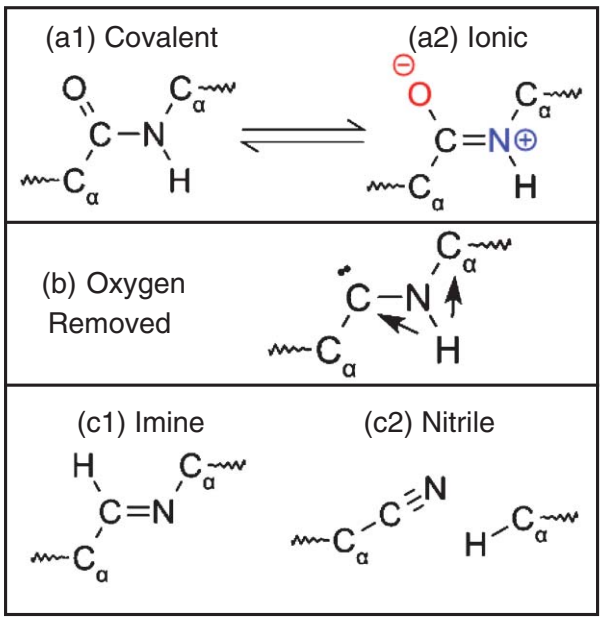

FIG. 4. Model for the dissociation of the amide bond, which is compatible with the absorption spectra at the N, O, and C 1s edges. The amide bond is a conjugated π system which can be viewed as a superposition of the "covalent" configuration (a1) and the "(zwitter)-ionic" configuration (a2). Configuration (a1) is required to observe a π^* orbital at the O 1s edge (Fig. 2) and Configuration (a2) to observe it at the N 1s edge (Fig. 1). (b) shows the intermediate state after removing the oxygen atom by irradiation. To repair the broken C=O bond, the H atom bonded to the N can migrate to one of the two adjacent carbon atoms (C or C_α), as indicated by two arrows. The two final reaction products are an imine in (c1) or a nitrile in (c2). They give rise to the two π^* peaks appearing at the N 1s absorption edge in Fig. 1.

"covalent" and a "(zwitter-)ionic" configuration. In the "covalent" configuration the orbital of the double-bond covers the C=O group, in the "ionic" configuration the $C{=}N^+$ group, and in the superposition it covers both. This leads to a single wave function which extends over all three atoms (N, C, O).

The O 1s spectra in Fig. 2 show an overall intensity reduction across the whole spectrum. This implies that the amide oxygen is released by the photochemical reaction, in agreement with the conclusion of previous studies.[9,29] Since the intensity is reduced not only for the π^* peak at $\approx$532.2 eV but also for the higher-lying σ^* manifold between 538 eV and 550 eV, the data cannot be explained by a conversion of π- to σ-bonded oxygen alone. There must be desorption of oxygen.

The loss of oxygen occurs at the same rate as the decrease of the π^* peak of the amide bond at the N 1s edge and the increase of the radiation-induced π^* doublet at the N 1s edge (not shown, see Ref. 32 for the decay and growth rates in cytochrome c). As with the results at the N 1s edge, the observations at the O 1s edge are common to the broad variety of amides covered in this study. Thus one has again a universal phenomenon.

The C 1s spectra in Fig. 3 are dominated by the π^* peak of the peptide bond at 288.1 eV in pristine samples. Irradiation quenches this peak, which is consistent with the findings at the N 1s and O 1s edges. Two new π^* features appear at lower energy, whose shape comes out more clearly in the difference spectrum. The arrow at 284.9 eV indicates a typical energy for the π^* peak of imines,[29,46,47] and the arrow at 286.5 eV denotes the characteristic energy of the π^* peak in nitriles.[29,48] The small peak at 287.7 eV in the difference spectrum is probably caused by a slight downward shift of the amide π^* peak. The C 1s edge tends to be less informative than the O 1s and N 1s edges because amides contain many other types of C atoms in addition to the C at the center of the amide bond. Some of these may exhibit their own photochemical reactions, for example, those in the amino acid residues. Therefore we refrain from a discussion of the smaller features in the C 1s spectra.

V. A MODEL THAT EXPLAINS THE SPECTROSCOPIC DATA

Several mechanisms have been considered to explain the low-lying π^* doublet created by irradiation of the amide bond. The observations on bacterial proteins were explained in terms of a de-oxygenation, followed by the formation of π-bonded carbon-nitride compounds.[9] De-oxygenation was inferred from the decrease of the π^* peak at the O 1s edge with irradiation, in agreement with our results. The formation of carbon-nitride compounds was suspected by analogy to N 1s absorption data from nitrogen-substituted graphite systems.

Studies of amino acids (rather than peptides) have also found the characteristic doublet of π^* transition at the N 1s edge as a result of irradiation,[29,44] even though pristine amino acids do not exhibit the π^* orbital characteristic of the amide bond.[29,37,38,44] A variety of pathways have been proposed[44] through which amino acids decompose upon irradiation, such as de-hydrogenation (de-protonation), de-hydration, de-carboxylation, de-carbonylation, and de-amination. In particular, de-protonation of amino acids was thought to be responsible for the formation of low-basicity nitrogen-containing functional substituents, such as imino (C=NH), cyano (C $\equiv$N), or amido ($CONH_2$). For the photochemistry of glycine,[29] a two-step model was proposed, in which an amino acid is initially polymerized to a peptide by irradiation, as identified by the appearance of the characteristic π^* peak of the amide bond at the N 1s edge. Further exposure results in the growth of the same π^* doublet that we observe for amides. The doublet was attributed to a combination of imine and nitrile,[29] which agrees with our assignment.

By combining the features in the C, N, and O 1s spectra of a wide variety of amides, we have developed a simple model for the radiation-induced decomposition of the amide bond, as shown in Fig. 4. First, the carbonyl oxygen is desorbed from the amide bond, leaving its carbon with a lone pair of electrons (Fig. 4(b)). Then a hydrogen is transferred from the amide nitrogen to one of the two carbon neighbors, either to the carbonyl carbon (C) or to the carbon of the amino acid residue (C_α). In the first case an imine is formed (Fig. 4(c1)) and in the second case a nitrile is formed. While the formation of an imine leaves the backbone intact, the formation of a nitrile involves breaking the N-C_α bond and terminating the C_α with the H (Fig. 4(c2)). While Fig. 4(b) is a natural intermediate step, we cannot rule out other intermediate configurations.

This model is consistent with the observed C, N, and O 1s spectra. It is universal, since it depends only upon the four atoms involved in the amide bond (C, N, O, H). The

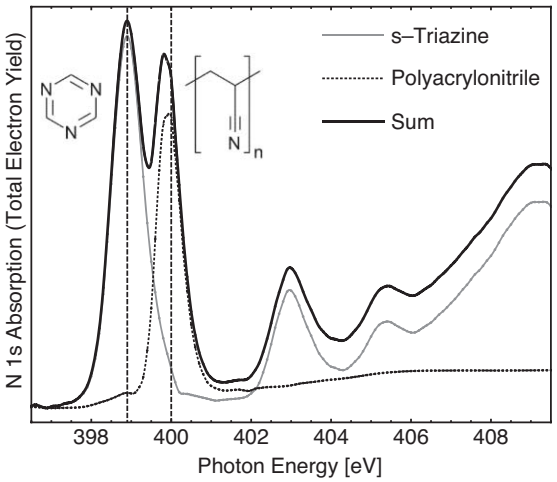

FIG. 5. N 1s absorption spectra of an imine and a nitrile, the two reaction products of the mechanism shown in Fig. 4. Their sum approximates the π^* doublet seen in Fig. 1 after irradiation, with dashed vertical lines indicating the average peak positions in Fig. 1. The data for s-triazine are from Apen *et al*. (Ref. 49).

structure of the amino acid residues has little influence, since the C_α atom is not involved in the amide bond. Interactions with neighboring molecules or different polymer strands are possible, for example via hydrogen bonding or dielectric screening. However, they cause only small core level shifts of a few tenths of an eV, as one can infer from the variation between the π^* peak positions in different compounds in Fig. 1.

To simulate the N 1s absorption spectrum resulting from this model we have added the spectrum of an imine and a nitrile in Fig. 5. Their superposition approximates the doublets seen in Fig. 1 reasonably well. The actual branching ratio of the two reactions is not as close to 1:1 as the π^* peak heights seem to indicate. The photoabsorption cross section of the nitrile π^* peak is significantly larger than that of the imine, judging from its much larger π^*/σ^* intensity ratio (not shown). Therefore, we conclude that there actually is significantly less nitrile than imine, in agreement with a previous finding for irradiated amino acids.[29]

VI. CONSIDERATION OF OTHER MODELS VIA REFERENCE COMPOUNDS

Even though the proposed model is able to explain the spectroscopic results, it is prudent to consider other proposed or conceivable models and investigate their expected fingerprints in the absorption spectra. Therefore we have investigated a large variety of reference compounds that might exhibit low-lying π^* orbitals (see Fig. 6). Since the amide bond contains nitrogen, one can use the N 1s edge to eliminate a large number of chemical reactions that do not involve nitrogen. Furthermore, the amide bond contains only a single nitrogen atom, which leads to a single π^* peak for all the amides investigated in Fig. 1. The single N makes the appearance of two π^* peaks after bond breaking quite a surprise. One can conceive several mechanisms to lead to a doublet at the N 1s edge:

(1) Two inequivalent N atoms are involved (see Figs. 6(d), 6(e), 6(h), and 6(i)). Since the amide bond contains only one N atom, one has to invoke either two different reaction pathways or the involvement of a second N atom in a neighbor molecule, e.g., via cross-linking, a common process in organic photochemistry.[2] Natural partner sites for cross-linking of polyamides are established by the hydrogen-bonds between adjacent amide groups: >C=O···H–N<.

(2) A single N atom is π-bonded to a larger conjugated π-system with several π^* levels. However, the higher π^* levels tend to have lower intensities (not shown).

(3) The degeneracy of the two orthogonal π^* orbitals of a triple-bonded nitrile is removed by coupling a planar π-system (see Fig. 6(c)).

(4) Two tautomers are involved, i.e., an amide can become an imidic acid by moving the H from the N to the O (see Figs. 6(h) and 6(i)). This is accompanied by an interchange of a single bond with a double bond. A similar bond swap can occur between an amine and an adjacent imine sharing a C atom, such as in Fig. 6(e). Only the dominant configuration is shown. The other has NH everywhere.

Even after identifying an explanation for the doublet, one still has to satisfy the constraints provided by the characteristic splitting of 1.1 eV and the intensity ratio of approximately 1:1.

In the following we will discuss the N 1s spectra in Fig. 6 from compounds which were selected as candidates for explaining the N 1s spectrum of the photochemical reaction and in particular the two low-lying π^* orbitals.

Figure 6(a), tris-pyridil triazine (π^* peak at 398.6 eV): This compound is representative of imine bonds in large N=C π-systems, as suggested previously.[9] These should have low-lying π^* orbitals according to the criteria developed above. That is indeed the case. The prominent π^* peak at 398.6 eV lies lower than most of the other π^* peaks in Fig. 6. This is close to the π^* peak of smaller imine systems, such as pyridine (398.8 eV),[47] pyrimidine (398.8 eV),[46,47] pyrazine (398.8 eV),[46,47] and s-triazine (398.9 eV).[47,49] We observe a similar value of 398.6 eV for the intermediate-sized triphenyltriazine (spectrum not shown). However, none of these compounds exhibits a splitting of the π^* peak, not even the larger π-systems which contain a manifold of π^* orbitals. This allows us to rule out a previous suspicion that graphitic carbon-nitride compounds are formed in radiation-damaged proteins[9] with a bonding configuration similar to nitrogen substituted graphite systems.[50] Other large aromatic systems, such as NTCDI (naphthalene tetracarboxylic diimide)[51] and porphyrins,[31] also show only a single LUMO peak at the N 1s edge, followed by much weaker peaks at ≈2 eV higher energy. Transitions into higher-lying π^* orbitals tend to become rapidly weaker in x-ray absorption spectroscopy.

Figure 6(b), polyacrylonitrile (π^* peak at 399.9 eV): The C ≡N bond contains two degenerate π^* orbitals which are produced by p_x, p_y orbitals perpendicular to the triple bond. This leads to a single peak at the N 1s edge, for example in acetonitrile[52] and polyacrylonitrile.[53]

Figure 6(c), the liquid crystal 8CB (π^* peaks at 399.1 and 399.9 eV): An energy splitting can be induced in the two degenerate C ≡N π^* orbitals by breaking the symme-

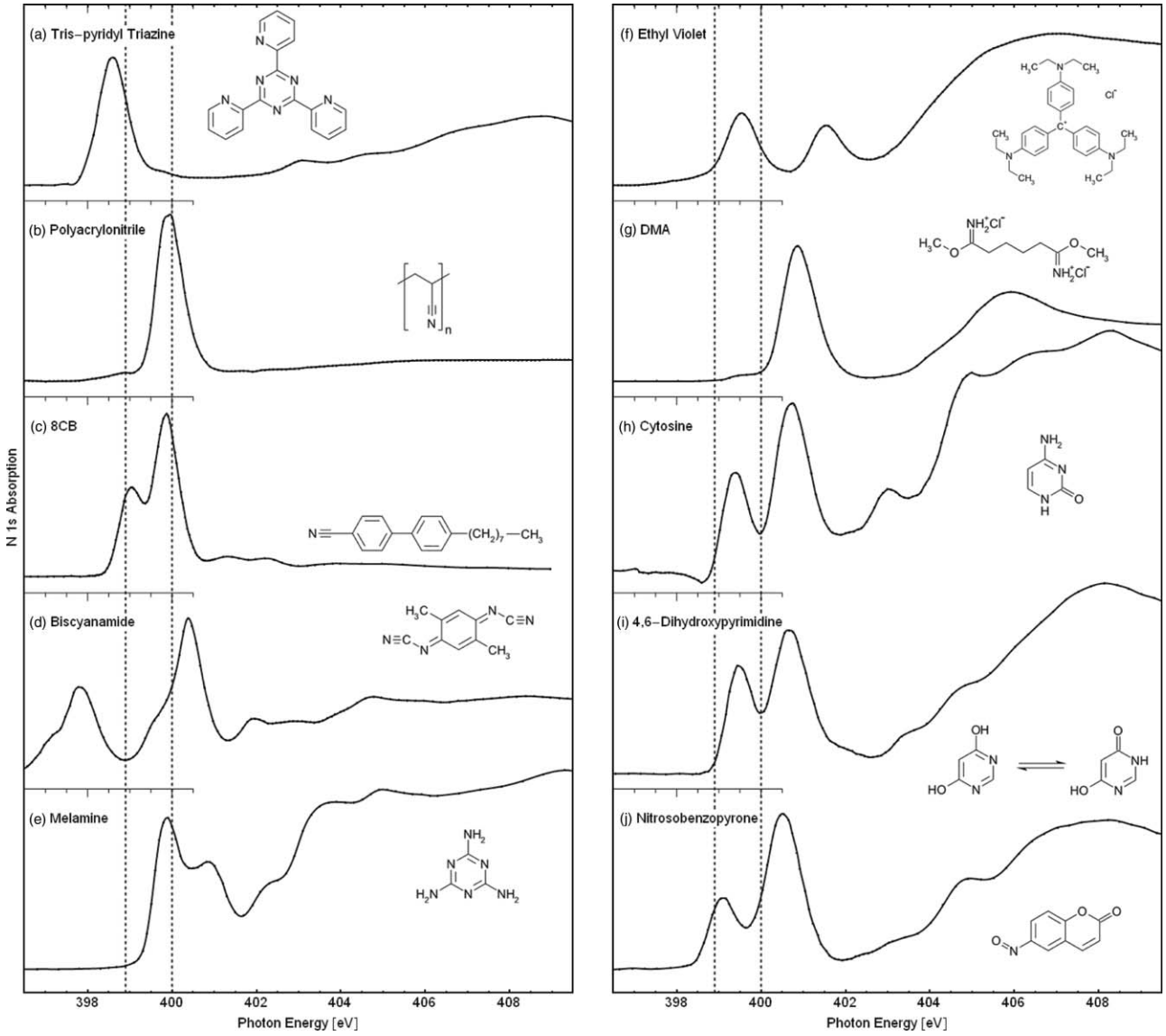

FIG. 6. N 1s absorption spectra of reference molecules for testing a variety of bond-breaking models. The two dashed vertical lines indicate the positions of the radiation-induced π^* orbitals in Fig. 1. (a) 2,4,6-Tris(2-pyridyl)-s-triazine, an example for the π-bonded C=N network. (b) Polyacrylonitrile (PAN), a nitrile with two degenerate π^* orbitals. (c) 8CB, a nitrile where the degeneracy is lifted by the attached phenyl ring. (d) Dimethyl cyclohexadiene diylidene biscyanamide, a molecule containing both nitrile and imine bonds. (e) Melamine, containing two types of N atoms. (f) Ethyl violet, a molecule with an overall positive charge. (g) Dimethyl adipimidate·2 HCl = DMA, a positively charged imine. (h) Cytosine, with three inequivalent N atoms, two of them π-bonded. (i) 4,6-Dihydroxypyrimidine, with two of its tautomers. (j) Nitrosobenzopyrone, where a single N atom produces two π^* peaks.

try between x and y. This can be achieved by coupling to an anisotropic ligand, such as a π-system consisting exclusively of p_x orbitals. Examples are acrylonitrile,[54] benzonitrile,[55] 9-cyanoanthracene,[53] and 5CB.[56,57] Our N 1s spectrum of 8CB shows the characteristic doublet of low-lying π^* peaks observed in all these nitriles.

Figure 6(d), dimethyl cyclohexadiene diylidene biscyanamide (π^* peaks at 397.8 and 400.4 eV): This molecule contains π^* orbitals of both imine and nitrile, plus an aromatic C ring. The interaction between these π systems leads to a complex manifold of π^* orbitals, including some at very low energy.

Figure 6(e), melamine (π^* peaks at 399.9 and 400.9 eV): Melamine contains two types of N atoms with different N 1s core level binding energies. The inner N atoms are π-bonded as imine inside the triazine ring. The outer N atoms are nominally in a σ-bonded amine configuration, which should not produce a low-lying π^* orbital. A closer look at the calculated charge distribution of the LUMO (Ref. 58) reveals that the π^*-system of the LUMO extends out of the triazine ring onto the outer N atoms, thereby encompassing both types of N atoms. Thus one can have two transitions from both N 1s core levels into the same LUMO. Indeed, XPS data of melamine-formaldehyde resins have been interpreted in terms of an imine nitrogen (=N–) with 398.4 eV binding energy and an amine nitrogen (–NH–) with 399.5 eV.[59] The XPS splitting of 1.1 eV agrees with our NEXAFS splitting of 1.0 eV at the N 1s edge (Fig. 6(b)) within the accuracy of the XPS data. Although melamine is amenable to tautomerism, the configuration shown in Fig. 6 is dominant in the solid phase.[60]

Figure 6(f), ethyl violet (a.k.a. gentian violet, π^* peaks at 399.6 and 401.6 eV): Ethyl violet exhibits a doublet

despite the equivalence of the three N atoms. The inset shows the dominant configuration with the positive charge residing on the central carbon atom and on the phenyl rings. A second configuration has the positive charge on one of the three N atoms. The situation is similar to that in malachite green, whose electronic structure has been investigated in detail.[61] The configurations containing N^+ are energetically less favorable, since N is more electronegative than C. In the absence of a more thorough theoretical study of ethyl violet it is difficult to make a clear assignment for the two observed π^* transitions. Tentatively one may associate the lower π^* peak at 399.6 eV with neutral N and the upper π^* peak at 401.6 eV with N^+, because the N 1s core level has a higher binding energy in N^+. An analogous shift (from 398.9 eV to 400.4 eV) has been observed with pyridine groups in poly(4-vinylpyridine) in solution when going from neutral N to protonated N at *p*H 2.5.[62]

Figure 6(g), dimethyl adipimidate·2 HCl = DMA (π^* peak at 400.9 eV): The dominant configuration $>C{=}N^+H_2$ represents iminium. HCl is separated into H^+ and Cl^- and the proton becomes attached to the NH group. Only a single π^* peak is observed, like for many imine compounds ranging from pyridine to the extended π-bonded network in Fig. 6(a) . Compared to imines, the positive charge of iminium increases the binding energy of the N 1s core level and so increases the transition energy. Thus, neither iminium nor imine alone lead to a promising route towards explaining a π^* doublet.

Figure 6(h), cytosine (π^* peaks at 399.4 and 400.7 eV): This nucleotide base exhibits a doublet of π^* orbitals. It contains three inequivalent N atoms in amine, imine, and amide configurations. The latter two produce π^* orbitals.

Figure 6(i), 4,6-dihydroxypyrimidine (π^* peaks at 399.5 and 400.7 eV): This is an example where several tautomers may coexist, i.e., the H can be attached either to the N or to the O atom of the amide bond (see the situation D listed above). In addition, one can have the ionic and covalent configurations discussed with the amide bond in Figs. 4(a1) and 4(a2). Here we have two amide bonds in one molecule, which allow for several combinations (compare Ref. 63). Furthermore, the stability of various tautomers changes when going from a solution to a molecular solid, where directional hydrogen bonds play a role in establishing the crystal lattice. Only two tautomers are shown in Fig. 6(h) to illustrate how a π^* doublet may be generated by tautomerism. The symmetric version would generate a single π^* peak, and the asymmetric version containing an amide and an imidic acid would generate two π^* peaks. Such effects have been observed by x-ray absorption and XPS,[64] with a splitting of 1.0 eV in the N 1s binding energy between -OH and -NH tautomers.

Figure 6(j), 6-nitroso-1,2-benzopyrone (π^* peaks at 399.1 and 400.5 eV): This nitroso compound surprisingly exhibits a low-lying doublet, despite the fact that the molecule contains only one N atom. Even though the splitting of 1.4 eV is too large to explain the doublet in Fig. 1, and despite the presence of oxygen, the nitroso group is useful for demonstrating an additional mechanism for obtaining a low-lying doublet at the N 1s edge. Our tentative explanation is based on calculations for nitrosobenzene.[65] The two lowest unoccupied orbitals with significant amplitude at the nitroso group lie at –1.131 eV and 0.754 eV. Their energy difference of 1.885 eV is comparable to the splitting of 1.4 eV observed in nitrosobenzopyrone. Looking at the calculated wave functions, one finds that these two orbitals represent the bonding and antibonding combinations of a π^* orbital of benzene and a π^* orbital of NO. Since the uppermost π^* orbital of NO is singly occupied, the NO group can replace a H atom of benzene.

None of the reference compounds in Fig. 6 can explain all of the observed features of the broken amide bond. Some have only a single π^* peak at the N 1s edge (a, b, and g), some have a double peak with the wrong splitting (c, d, f, h, and j), some have a doublet at the wrong energy (e and i), and some still contain oxygen (g, h, i, and j).

VII. CONCLUSIONS AND OUTLOOK

In summary, we find that irradiation of amides by soft x-rays universally leads to a characteristic signature at the N 1s x-ray absorption edge. The π^* peak of the amide bond is replaced by a low-lying doublet of π^* peaks with a splitting of 1.1 eV. This signature is found for a wide range of amides, from small peptides to large proteins, as well as for polymers such as nylon. A systematic search is undertaken to identify possible reaction products that exhibit the same spectroscopic features, including previously proposed reaction products. Among many possible models that have been tested, only one is consistent with the spectroscopic results. This model consists of an initial desorption of O followed by a migration of H from the amide N to one of the neighbor C atoms. These two pathways lead to two different reaction products, an imine and a nitrile. Since an imine keeps the backbone intact and a nitrile leads to fragmentation, it would be interesting to verify these predictions by independent methods.

This finding has consequences beyond amides. It has been found that amino acids[29,44] and imides[33] can exhibit the same characteristic π^* doublet at the N 1s edge after irradiation, because they are first converted to an amide which then decays via the universal pattern.

In the future, it would be interesting to explore whether other types of radiation produce the same bond breaking pattern (for example electrons or ions). Our observation of the same reaction products over the photon energy range of 11–600 eV suggests that the initial photoexcitation process is less important than the decay processes which create a large number of secondary electrons per photon. Secondary electrons are produced by all kinds of ionizing radiation. They are able to populate the antibonding orbitals and thus initiate bond breaking (compare the role of electrons in the radiation damage work on DNA (Refs. 23 and 24)).

A related question is the role of radicals and ions created via fragmentation of waters of hydration by irradiation, a process that has been widely discussed as a potential cause of radiation damage in protein crystallography.

A further avenue of interest would be a theoretical investigation of how the H atom migrates from the N to one of the two nearby C atoms. That could explain the observed branching ratio between the imine and nitrile reaction products.

ACKNOWLEDGMENTS

We acknowledge helpful discussions with Dmitri Petrovykh, Thomas D. Clark, Adam Hitchcock, Michel Koch, Neville Richardson, P.U.P.A. Gilbert, Stephanie Hogendoorn, Robert Julian, Michael Nasse, and Carol Hirschmugl. This work was supported by the NSF under awards DMR-0520527 (MRSEC), DMR-0537588 (SRC), and by the DOE under Contract Nos. DE-FG02-01ER45917 (ALS end station) and DE-AC03-76SF00098 (ALS).

[1] P. R. Bergethon, *The Physical Basis of Biochemistry: The Foundations of Molecular Biophysics* (Springer, New York, 1998), Chap. 23.
[2] J. D. Coyle, *Introduction to Organic Photochemistry* (Wiley, New York, 1989).
[3] A. Cefalas and E. Sarantopoulou, Microelectron. Eng. **53**, 465 (2000).
[4] M. Weik, R. B. G. Ravelli, G. Kryger, S. McSweeney, M. L. Raves, M. Harel, P. Gros, I. Silman, J. Kroon, and J. L. Sussman, Proc. Natl. Acad. Sci. U.S.A. **97**, 623 (2000).
[5] P. O'Neill, D. L. Stevens, and E. F. Garman, J. Synchrotron Radiat. **9**, 329 (2002).
[6] J. Yano, J. Kern, K.-D. Irrgang, M. J. Latimer, U. Bergmann, P. Glatzel, Y. Pushkar, J. Biesiadka, B. Loll, K. Sauer, J. Messinger, A. Zouni, and V. K. Yachandra, Proc. Natl. Acad. Sci. U.S.A. **102**, 12047 (2005).
[7] J. B. Fenn, M. Mann, C. K. Meng, S. F. Wong, and C. M. Whitehouse, Science **246**, 64 (1989).
[8] D. Sayre, J. Kirz, R. Feder, D. Kim, and E. Spiller, Ultramicroscopy **2**, 337 (1976–1977).
[9] A. Kade, D. V. Vyalikh, S. Danzenbächer, K. Kummer, A. Blüher, M. Mertig, A. Lanzara, A. Scholl, A. Doran, and S. L. Molodtsov, J. Phys. Chem. B **111**, 13491 (2007).
[10] J. C. H. Spence, *High-Resolution Electron Microscopy* (Oxford University Press, New York, 2003), Chap. 6.
[11] J. Wang, C. Morin, L. Li, A. Hitchcock, A. Scholl, and A. Doran, J. Electron Spectrosc. Relat. Phenom. **170**, 25 (2009).
[12] T. Coffey, S. G. Urquhart, and H. Ade, J. Electron Spectrosc. Relat. Phenom. **122**, 65 (2002).
[13] M. Said, B. Dingwall, A. Gupta, A. Seyam, G. Mock, and T. Theyson, Adv. Space Res. **37**, 2052 (2006).
[14] M. Diepens and P. Gijsman, Polym. Degrad. Stab. **92**, 397 (2007).
[15] B. Basile, A. Lazcano, and J. Oró, Adv. Space Res. **4**, 125 (1984).
[16] M. Lattelais, O. Risset, J. Pilme, F. Pauzat, Y. Ellinger, F. Sirotti, M. Silly, P. Parent, and C. Laffon, Intl. J. Quantum Chem. **111**, 1163 (2011).
[17] W. M. Garrison and B. M. Weeks, Radiat. Res. **17**, 341 (1962).
[18] J. Coyle, Pure Appl. Chem. **60**, 941 (1988).
[19] R. Weinkauf, P. Schanen, A. Metsala, E. W. Schlag, M. Bürgle, and H. Kessler, J. Phys. Chem. **100**, 18567 (1996).
[20] N. R. Forde, L. J. Butler, and S. A. Abrash, J. Chem. Phys. **110**, 8954 (1999).
[21] R. N. Grewal, H. El Aribi, A. G. Harrison, K. W. M. Siu, and A. C. Hopkinson, J. Phys. Chem. B **108**, 4899 (2004).
[22] S. J. George, J. Fu, Y. Guo, O. B. Drury, S. Friedrich, T. Rauchfuss, P. I. Volkers, J. C. Peters, V. Scott, S. D. Brown, C. M. Thomas, and S. P. Cramer, Inorg. Chim. Acta **361**, 1157 (2008).
[23] B. Boudaïffa, P. Cloutier, D. Hunting, M. A. Huels, and L. Sanche, Science **287**, 1658 (2000).
[24] H. Abdoul-Carime, S. Gohlke, and E. Illenberger, Phys. Rev. Lett. **92**, 168103 (2004).
[25] D. Menzel and R. Gomer, J. Chem. Phys. **41**, 3311 (1964).
[26] P. Redhead, Can. J. Phys. **42**, 886 (1964).
[27] M. L. Knotek and P. J. Feibelman, Phys. Rev. Lett. **40**, 964 (1978).
[28] P. Avouris and R. Walkup, Annu. Rev. Phys. Chem. **40**, 173 (1989).
[29] R. G. Wilks, J. B. MacNaughton, H.-B. Kraatz, T. Regier, R. I. R. Blyth, and A. Moewes, J. Phys. Chem. A **113**, 5360 (2009).
[30] S. Myneni, Y. Luo, L. Å Näslund, M. Cavalleri, L. Ojamäe, H. Ogasawara, A. Pelmenschikov, P. Wernet, P. Väterlein, C. Heske, Z. Hussain, L. G. M. Pettersson, and A. Nilsson, J. Phys.: Condens. Matter **14**, L213 (2002).
[31] P. L. Cook, X. Liu, W. Yang, and F. J. Himpsel, J. Chem. Phys. **131**, 194701 (2009).
[32] P. L. Cook, P. S. Johnson, X. Liu, A.-L. Chin, and F. J. Himpsel, The J. Chem. Phys. **131**, 214702 (2009).
[33] P. S. Johnson, P. L. Cook, X. Liu, W. Yang, Y. Bai, N. L. Abbott, and F. J. Himpsel, "Multi-step photodissociation of an imide" (unpublished).
[34] R. N. S. Sodhi and C. E. Brion, J. Electron Spectrosc. Relat. Phenom. **34**, 363 (1984).
[35] H. Fischer, I. Polikarpov, and A. F. Craievich, Protein Sci. **13**, 2825 (2004).
[36] R. Giebler, B. Schulz, J. Reiche, L. Brehmer, M. Wühn, C. Wöll, A. P. Smith, S. G. Urquhart, H. W. Ade, and W. E. S. Unger, Langmuir **15**, 1291 (1999).
[37] M. L. Gordon, G. Cooper, C. Morin, T. Araki, C. C. Turci, K. Kaznatcheev, and A. P. Hitchcock, J. Phys. Chem. A **107**, 6144 (2003).
[38] G. Cooper, M. Gordon, D. Tulumello, C. Turci, K. Kaznatcheev, and A. P. Hitchcock, J. Electron Spectrosc. Relat. Phenom. **137–140**, 795 (2004).
[39] X. Liu, C.-H. Jang, F. Zheng, A. Jürgensen, J. D. Denlinger, K. A. Dickson, R. T. Raines, N. L. Abbott, and F. J. Himpsel, Langmuir **22**, 7719 (2006).
[40] P. Leinweber, J. Kruse, F. L. Walley, A. Gillespie, K.-U. Eckhardt, R. I. R. Blyth, and T. Regier, J. Synchrotron Radiat. **14**, 500 (2007).
[41] J. Stewart-Ornstein, A. P. Hitchcock, D. Hernández Cruz, P. Henklein, J. Overhage, K. Hilpert, J. D. Hale, and R. E. W. Hancock, J. Phys. Chem. B **111**, 7691 (2007).
[42] Y. Zubavichus, A. Shaporenko, M. Grunze, and M. Zharnikov, J. Phys. Chem. B **111**, 9803 (2007).
[43] Y. Zubavichus, A. Shaporenko, M. Grunze, and M. Zharnikov, J. Phys. Chem. B **112**, 4478 (2008).
[44] Y. Zubavichus, M. Zharnikov, A. Shaporenko, O. Fuchs, L. Weinhardt, C. Heske, E. Umbach, J. D. Denlinger, and M. Grunze, J. Phys. Chem. A **108**, 4557 (2004).
[45] G. R. Carruthers, Appl. Opt. **10**, 1461 (1971).
[46] S. Aminpirooz, L. Becker, B. Hillert, and J. Haase, Surf. Sci. **244**, L152 (1991).
[47] G. Vall-llosera, B. Gao, A. Kivimäki, M. Coreno, J. Álvarez Ruiz, M. de Simone, H. Ågren, and E. Rachlew, J. Chem. Phys. **128**, 044316 (2008).
[48] O. Dhez, H. Ade, and S. G. Urquhart, J. Electron Spectrosc. Relat. Phenom. **128**, 85 (2003).
[49] E. Apen, A. P. Hitchcock, and J. L. Gland, J. Phys. Chem. **97**, 6859 (1993).
[50] I. Shimoyama, G. Wu, T. Sekiguchi, and Y. Baba, Phys. Rev. B **62**, R6053 (2000).
[51] M. Ruiz-Osés, T. Kampen, N. González-Lakunza, I. Silanes, P. M. Schmidt-Weber, A. Gourdon, A. Arnau, K. Horn, and J. E. Ortega, ChemPhysChem **8**, 1722 (2007).
[52] S. Carniato, R. Taïeb, E. Kukk, Y. Luo, and B. Brena, J. Chem. Phys. **123**, 214301 (2005).
[53] O. Plashkevych, A. Snis, L. Yang, H. Ågren, and S. F. Matar, Phys. Scr. **63**, 70 (2001).
[54] J. J. Gallet, F. Bournel, S. Kubsky, G. Dufour, F. Rochet, and F. Sirotti, J. Electron Spectrosc. Relat. Phenom. **122**, 285 (2002).
[55] S. Carniato, V. Ilakovac, J.-J. Gallet, E. Kukk, and Y. Luo, Phys. Rev. A **71**, 022511 (2005).
[56] K. Weiss, C. Wöll, and D. Johannsmann, J. Chem. Phys. **113**, 11297 (2000).
[57] N. Ballav, B. Schüpbach, O. Dethloff, P. Feulner, A. Terfort, and M. Zharnikov, J. Am. Chem. Soc. **129**, 15416 (2007).
[58] V. Chis, G. Mile, R. Stiufiuc, N. Leopold, and M. Oltean, J. Mol. Struc. **924–926**, 47 (2009).
[59] A. Derylo-Marczewska, J. Goworek, S. Pikus, E. Kobylas, and W. Zgrajka, Langmuir **18**, 7538 (2002).
[60] I. M. Klotz and T. Askounis, J. Am. Chem. Soc. **69**, 801 (1947).
[61] D. H. Nguyen, S. C. DeFina, W. H. Fink, and T. Dieckmann, J. Am. Chem. Soc. **124**, 15081 (2002).
[62] S. Fujii, S. P. Armes, T. Araki, and H. Ade, J. Am. Chem. Soc. **127**, 16808 (2005).
[63] A. Katrusiak and A. Katrusiak, Org. Lett. **5**, 1903 (2003).
[64] E. Ito, H. Oji, T. Araki, K. Oichi, H. Ishii, Y. Ouchi, T. Ohta, N. Kosugi, Y. Maruyama, T. Naito, T. Inabe, and K. Seki, J. Am. Chem. Soc. **119**, 6336 (1997).
[65] H.-J. Freund, R. W. Bigelow, B. Börsch-Pulm, and H. Pulm, Chem. Phys. **94**, 215 (1985).